Adaptive Control of a Quadrotor UAV Transporting a Cable-Suspended Load with Unknown Mass

Shicong Dai, Taeyoung Lee, and Dennis S. Bernstein

***Abstract*— We design an adaptive controller for a quadrotor UAV transporting a mass-point payload connected by a flexible cable modeled as serially-connected rigid links. The mass of the payload is uncertain. The objective is to transport the payload to a desired position while aligning the links along the vertical direction from an arbitrary initial condition. A fixed-gain nonlinear proportional-derivative controller is presented to achieve desired performance for a nominal payload mass, and a retrospective cost adaptive controller is used to compensate for the payload mass uncertainty. This approach is illustrated by numerical examples.**

I. Introduction

Quadrotor unmanned aerial vehicles have simple mechanical structures, but they have the desirable capabilities of hovering and vertical take-off and landing. They have been envisaged for various applications, including mobile sensor network, aerial photography, and educational research. In particular, several aggressive maneuvers have been demonstrated by utilizing their high thrust-to-weight ratio [1]–[3].

These properties are also particularly useful for autonomous load transportation. Aerial transportation of a cable-suspended load has been studied traditionally for helicopters [4], [5]. Small-size single or multiple autonomous vehicles are considered for load transportation and deployment [6]–[8].

However, these results are based on a simplified dynamic model, where the dynamic effects of the payload to the quadrotor are approximated by unstructured disturbances without considering the nontrivial dynamic coupling between the payload and the quadrotor. As such, they are not suitable for rapid load transportation, where the dynamics of the payload can be excited significantly.

Recently, a coordinate-free form of the equations of motion are developed for the integrated dynamics of a quadrotor, cable, and payload. Based on this complete dynamic model, geometric tracking control systems are constructed for a single quadrotor transporting a cable-suspended point mass [9], and for a cooperative group of quadrotors transporting a common payload connected by multiple cables, while controlling the relative formation among them [10]. It is further generalized for the case where a payload is connected to a quadrotor via a flexible cable that can be deformed arbitrarily [11].

These approaches incorporate the dynamic coupling between the payload and the quadrotor explicitly in control system design and stability analysis. However, it is assumed that the mass property of the payload is exactly known. In practical applications of autonomous aerial load transportation, where various payloads with a broad range of mass properties must be delivered repeatedly at low cost, it is desirable that the quadrotor can transport the payload autonomously without relying on the exact knowledge of the payload mass.

The objective of this paper is to design an adaptive control system for a quadrotor that delivers a cable-suspended payload without a prior knowledge of the payload mass. The cable is modeled as a serially-connected rigid links and the payload is modelled as a point-mass. Retrospective cost adaptive control (RCAC) is constructed to guarantee excellent performances while compensating for the payload mass uncertainty. In short, the main contribution of this paper is the development of an adaptive control for the complete dynamics of a quadrotor transporting a cable-suspended payload with unknown mass.

RCAC is a direct adaptive control technique that requires limited modeling information [12]–[14]. The algorithm has been applied to various complex dynamic systems, such as aircraft [14], multiple linkages [15], [16], and spacecraft attitude dynamics [17], [18]. RCAC is based on optimizing the retrospective cost performance, which is derived from fictitiously applying the current controller in the past. This strategy enable RCAC to control a system based on its input-output relation instead of a complex state-space model. This feature is essential in the development of the proposed adaptive control system due to the complexity of the dynamic model. In this paper, we use the impulse response of the quadrotor with a fixed-gain controller in the loop to apply RCAC.

This paper is organized as follows. A dynamic model is presented and RCAC algorithm is described at Section II, and III, respectively. The proposed RCAC for quadrotor is presented at Section IV, which is followed by numerical examples at Section V.

II. Dynamic Model of a Quadrotor with a Flexible Cable

Consider a quadrotor UAV with a payload that is connected by a chain of n links, as illustrated at Fig. 1. The

Shicong Dai is with School of Automation Science and Electrical Engineering, Beihang University, Beijing, 100191 daibluewater@gmail.com

Taeyoung Lee is with Department of Mechanical and Aerospace Engineering, The George Washington University, Washington, DC 20052 tylee@gwu.edu

Dennis S. Bernstein is with Department of Aerospace Engineering, University of Michigan, Ann Arbor, MI 48109 dsbaero@umich.edu

*This research has been supported in part by NSF under the grant CMMI-1243000 (transferred from 1029551), CMMI-1335008, and CNS-1337722.

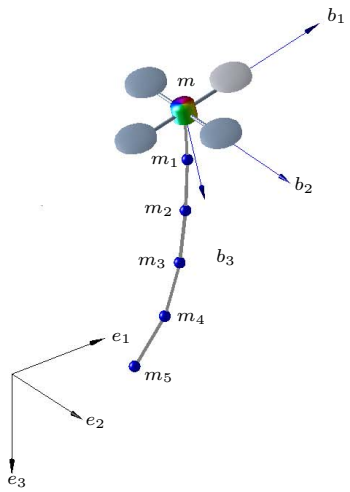

Fig. 1. Quadrotor UAV with a cable-suspended load. The cable is modeled as a serial connection of arbitrary number of links (We show 5 links here as an example). It is assumed that the mass of the payload is unknown.

inertial frame is defined by the unit vectors $e_1 \triangleq [1\ 0\ 0]^{\mathrm{T}}$, $e_2 \triangleq [0\ 1\ 0]^{\mathrm{T}}$, and $e_3 \triangleq [0\ 0\ 1]^{\mathrm{T}} \in \mathbb{R}^3$, and the third axis e_3 corresponds to the direction of gravity. Define a body-fixed frame $\{\vec{b}_1, \vec{b}_2, \vec{b}_3\}$ whose origin is located at the center of mass of the quadrotor, and its third axis $\vec{b}_3$ is aligned with the axis of symmetry of the quadrotor.

The location of the mass center, and the attitude of the quadrotor are denoted by $x \triangleq [x_1\ x_2\ x_3]^{\mathrm{T}} \in \mathbb{R}^3$ and $R \in \mathsf{SO(3)}$, respectively, where the special orthogonal group is $\mathsf{SO(3)} \triangleq \{R \in \mathbb{R}^{3\times 3} \,|\, R^T R = I_3,\ \det R = 1\}$. A rotation matrix represents the linear transformation of a representation of a vector from the body-fixed frame to the inertial frame.

The dynamic model of the quadrotor is identical to [1]. The mass and the inertia matrix of the quadrotor are denoted by $m \in \mathbb{R}$ and $J \in \mathbb{R}^{3\times 3}$, respectively. The quadrotor can generate a thrust $-fRe_3 \in \mathbb{R}^3$ relative to the inertial frame, where $f \in \mathbb{R}$ is the total thrust magnitude. It also generates a moment $M \triangleq [M_1\ M_2\ M_3]^{\mathrm{T}} \in \mathbb{R}^3$ relative to the body-fixed frame. The pair (f, M) is considered as the control input of the quadrotor.

Let $q_i \in \mathsf{S}^2$ be the unit vector representing the direction of the i-th link, measured outward from the quadrotor toward the payload, where the two-sphere is the manifold of unit-vectors in $\mathbb{R}^3$, i.e., $\mathsf{S}^2 \triangleq \{q \in \mathbb{R}^3 \,|\, \|q\| = 1\}$. For simplicity, we assume that the mass of each link is concentrated at the outboard end of the link, and the point where the first link is attached to the quadrotor corresponds to the mass center of the quadrotor. The mass and length of the i-th link are defined by m_i and $l_i \in \mathbb{R}$, respectively. Thus, the mass of the payload corresponds to m_n, which is unknown. The corresponding configuration manifold of this system is $\mathbb{R}^3 \times \mathsf{SO(3)} \times (\mathsf{S}^2)^n$.

To derive the kinematics equations, let $\Omega \triangleq [\Omega_1\ \ \Omega_2\ \ \Omega_3]^{\mathrm{T}} \in \mathbb{R}^3$ be the angular velocity of the quadrotor represented relative to the body-fixed frame, and let $\omega_i \in \mathbb{R}^3$ be the angular velocity of the i-th link represented relative to the inertial frame. The angular velocity is normal to the direction of the link, i.e., $q_i \cdot \omega_i = 0$. The kinematics equations are given by

$$\dot{R} = R\hat{\Omega}, \tag{1}$$

$$\dot{q}_i = \omega_i \times q_i = \hat{\omega}_i q_i, \tag{2}$$

where the hat map $\hat{\cdot} : \mathbb{R}^3 \to \mathfrak{so}(3)$ is defined such that $\hat{x}y = x \times y$ for $x, y \in \mathbb{R}^3$, and the lie algebra is defined as $\mathfrak{so}(3) = \{A \in \mathbb{R}^{3\times 3} \,|\, A = -A^T\}$. The inverse of the hat map is denoted by $\vee : \mathfrak{so}(3) \to \mathbb{R}^3$. The 2-norm of a matrix A is denoted by $\|A\|$, and the dot product is denoted by $x \cdot y = x^T y$.

A. Euler-Lagrange equations

Consider a quadrotor with a cable-suspended payload, the Euler-Lagrange equations on $\mathbb{R}^3 \times \mathsf{SO(3)} \times (\mathsf{S}^2)^n$ are given by [11]:

$$J\dot{\Omega} + \hat{\Omega}J\Omega = M \tag{3}$$

and

$$\begin{bmatrix} m_{00} & m_{01} & m_{02} & \cdots & m_{0n} \\ -\hat{q}_1^2 m_{10} & m_{11} I_3 & -m_{12}\hat{q}_1^2 & \cdots & -m_{1n}\hat{q}_1^2 \\ -\hat{q}_2^2 m_{20} & -m_{21}\hat{q}_2^2 & m_{22} I_3 & \cdots & -m_{2n}\hat{q}_2^2 \\ \vdots & \vdots & \vdots & & \vdots \\ -\hat{q}_n^2 m_{n0} & -m_{n1}\hat{q}_n^2 & -m_{n2}\hat{q}_n^2 & \cdots & m_{nn} I_3 \end{bmatrix} \begin{bmatrix} \ddot{x} \\ \ddot{q}_1 \\ \ddot{q}_2 \\ \vdots \\ \ddot{q}_n \end{bmatrix} = \begin{bmatrix} -fRe_3 + m_{00} g e_3 \\ -\|\dot{q}_1\|^2 m_{11} q_1 - \sum_{a=1}^{n} m_a g l_1 \hat{q}_1^2 e_3 \\ -\|\dot{q}_2\|^2 m_{22} q_2 - \sum_{a=2}^{n} m_a g l_2 \hat{q}_2^2 e_3 \\ \vdots \\ -\|\dot{q}_n\|^2 m_{nn} q_n - m_n g l_n \hat{q}_n^2 e_3 \end{bmatrix}, \tag{4}$$

where the inertia values are given by

$$m_{00} = m + \sum_{i=1}^{n} m_i, \quad m_{0i} = \sum_{a=i}^{n} m_a l_i, \quad m_{i0} = m_{0i},$$

$$m_{ij} = \left(\sum_{a=\max\{i,j\}}^{n} m_a \right) l_i l_j. \tag{5}$$

These provide a coordinate-free form of the equations of motion for the presented quadrotor UAV that is uniformly defined for an arbitrary number of links n, and that is globally defined on the nonlinear configuration manifold. Compared with equations of motion derived in terms of local coordinates, such as Euler angles, these provide a compact form of equations that are suitable for control system design.

B. Actuator Model

We assume that the torque generated by each propeller is directly proportional to its thrust. Since that the first and the third propellers rotate clockwise, and the second and the fourth propellers rotate counterclockwise, when the propellers are generating a positive thrust f_i along $-\vec{b}_3$, the torque generated by the i-th propeller can be written as $c_{\tau f} f_i$

[19], [20]. Under these assumptions, the total thrust f and the total moment $M \triangleq [M_1\ M_2\ M_3]^{\mathrm{T}}$ can be written as

$$\begin{bmatrix} f \\ M_1 \\ M_2 \\ M_3 \end{bmatrix} = \begin{bmatrix} 1 & 1 & 1 & 1 \\ 0 & -d & 0 & d \\ d & 0 & -d & 0 \\ -c_{\tau f} & c_{\tau f} & -c_{\tau f} & c_{\tau f} \end{bmatrix} \begin{bmatrix} f_1 \\ f_2 \\ f_3 \\ f_4 \end{bmatrix}, \quad (6)$$

where d is the distance from the mass center of the quadrotor to the center of each rotor in the $\vec{b}_1$, $\vec{b}_2$ plane, and f_i is the thrust of the i-th propeller.

III. RCAC Algorithm Statement

Consider the MIMO system

$$x(k+1) = Ax(k) + Bu(k) + D_1 w(k), \quad (7)$$

$$z(k) = Cx(k) + D_2 w(k), \quad (8)$$

where $x(k) \in \mathbb{R}^{l_x}$, $z(k) \in \mathbb{R}^{l_z}$, $u(k) \in \mathbb{R}^{l_u}$, and $w(k) \in \mathbb{R}^{l_w}$.

For $n_{\mathrm{f}} > 0$, $z(k)$ is given by

$$z(k) = CA^{n_{\mathrm{f}}} x(k-n_{\mathrm{f}}) + D_2 w(k) + \sum_{i=1}^{n_{\mathrm{f}}} CA^{i-1} D_1 w(k-i) + \sum_{i=1}^{n_{\mathrm{f}}} H_i u(k-i), \quad (9)$$

where $H_i \triangleq CA^{i-1}B$.

The signal $w(k)$ represents either disturbances to be rejected or commands to be followed, or both. The goal is to develop an adaptive output feedback controller that minimizes the performance variable z in the presence of the unknown exogenous signal $w(k)$ with limited modeling information about (7) and (8). The required modeling data is described below.

A. Control Law

We use a strictly proper time-series controller of order n_{c} of the form

$$u(k) = \mathcal{M}_0(k) + \sum_{i=1}^{n_{\mathrm{c}}} \mathcal{M}_i(k) u(k-i) + \sum_{i=1}^{n_{\mathrm{c}}} \mathcal{N}_i(k) z(k-i), \quad (10)$$

where $\mathcal{M}_0(k) \in \mathbb{R}^{l_u}$ and, for all $i = 1, \ldots, n_{\mathrm{c}}$, $\mathcal{M}_i(k) \in \mathbb{R}^{l_u \times l_u}$ and $\mathcal{N}_i(k) \in \mathbb{R}^{l_u \times l_z}$. The controller (10) can be represented as

$$u(k) = \theta(k)\phi(k), \quad (11)$$

where

$$\theta(k) \triangleq [\mathcal{N}_1(k)\ \cdots\ \mathcal{N}_{n_{\mathrm{c}}}(k)\ \mathcal{M}_1(k)\ \cdots\ \mathcal{M}_{n_{\mathrm{c}}}(k)\ \mathcal{M}_0] \in \mathbb{R}^{l_u \times (n_{\mathrm{c}}(l_u+l_z)+1)} \quad (12)$$

and

$$\phi(k) \triangleq [z^{\mathrm{T}}(k-1)\ \cdots\ z^{\mathrm{T}}(k-n_{\mathrm{c}})\ u^{\mathrm{T}}(k-1)\ \cdots\ u^{\mathrm{T}}(k-n_{\mathrm{c}})\ 1]^{\mathrm{T}} \in \mathbb{R}^{n_{\mathrm{c}}(l_u+l_z)+1}. \quad (13)$$

B. Retrospective Performance

For $\hat{\theta} \in \mathbb{R}^{l_u \times n_{\mathrm{c}}(l_u+l_z)+1}$ and $n_{\mathrm{f}} \geq 1$, we define the *retrospective performance*

$$\hat{z}(\hat{\theta}, k) \triangleq z(k) + \sum_{i=1}^{n_{\mathrm{f}}} H_i[\hat{u}(k) - u(k-i)], \quad (14)$$

where

$$\hat{u}(k) \triangleq \hat{\theta}\phi(k) \quad (15)$$

is the retrospective control.

The retrospective performance $\hat{z}(\hat{\theta}, k)$ can be interpreted as the performance assuming that $\hat{\theta}$ was used in the past. Defining $\Theta(k) = \operatorname{vec} \theta(k) \in \mathbb{R}^{n_{\mathrm{c}} l_u (l_z+l_u)+l_u}$ and $\hat{\Theta} = \operatorname{vec} \hat{\theta} \in \mathbb{R}^{n_{\mathrm{c}} l_u (l_z+l_u)+l_u}$, it follows that

$$\begin{aligned} \hat{z}(\hat{\Theta}, k) &\triangleq z(k) + \sum_{i=1}^{n_{\mathrm{f}}} \Phi^{\mathrm{T}}(k)[\hat{\Theta} - \Theta(k-i)] \\ &= z(k) - \sum_{i=1}^{n_{\mathrm{f}}} \Phi^{\mathrm{T}}(k)\Theta(k-i)] + \Psi^{\mathrm{T}}(k)\hat{\Theta}, \end{aligned} \quad (16)$$

where, for all $i = 1, \ldots, n_{\mathrm{f}}$, $\Phi_i(k) \triangleq \phi(k-i) \otimes H_i^{\mathrm{T}} \in \mathbb{R}^{(n_{\mathrm{c}} l_u (l_z+l_u)+l_u) \times l_z}$ and $\Psi(k) \triangleq \sum_{i=1}^{n_{\mathrm{f}}} \Phi_i(k) \in \mathbb{R}^{(n_{\mathrm{c}} l_u (l_z+l_u)+l_u) \times l_z}$.

C. Cumulative Retrospective Cost Optimization

The cumulative retrospective cost function is defined by

$$\begin{aligned} J(\hat{\Theta}, k) \triangleq &\sum_{j=0}^{k} \lambda^{k-i} \hat{z}(\hat{\Theta}, k)^{\mathrm{T}} R_z \hat{z}(\hat{\Theta}, k) \\ &+ \lambda^k (\hat{\Theta} - \Theta(0))^{\mathrm{T}} R_\Theta (\hat{\Theta} - \Theta(0)), \end{aligned} \quad (17)$$

where $R_\Theta \in \mathbb{R}^{(n_{\mathrm{c}} l_u (l_z+l_u)+l_u) \times (n_{\mathrm{c}} l_u (l_z+l_u)+l_u)}$ and $R_z \in \mathbb{R}^{l_z}$ is positive definite, and $\lambda \in (0, 1]$ is the forgetting factor. The next result follows from standard recursive-least-squares theory [21].

Let $P(0) = R_\Theta^{-1}$ and $\Theta(0) \in \mathbb{R}^{(n_{\mathrm{c}} l_u (l_z+l_u)+l_u)}$. Then, for all $k \geq 0$, the unique global minimizer of (17) is given by $\hat{\Theta} = \Theta(k)$, where

$$\Theta(k+1) = \Theta(k) - \frac{P(k)\Psi(k)\hat{z}(\Theta(k), k)}{\lambda R_z^{-1} + \Psi^{\mathrm{T}}(k)P(k)\Psi(k)}, \quad (18)$$

$$P(k+1) = \frac{1}{\lambda}\left[P(k) - \frac{P(k)\Psi(k)\Psi^{\mathrm{T}}(k)P(k)}{\lambda R_z^{-1} + \Psi^{\mathrm{T}}(k)P(k)\Psi(k)}\right]. \quad (19)$$

IV. RCAC for Quadrotor Transporting a Cable-Suspended Load

Let $x_{\mathrm{p,d}} \in \mathbb{R}^3$ be the fixed desired location of the payload. We assume that all of the states of (1), (2), and (4) are measured. The control objective is to move a payload of uncertain mass m_n to $x_{\mathrm{p,d}}$ while aligning the links in the vertical direction. Note the position of the payload is given by $x_{\mathrm{p}} \triangleq [x_{\mathrm{p},1}\ x_{\mathrm{p},2}\ x_{\mathrm{p},3}] = x + \sum_{i=1}^{n} l_i q_i$.

Since x_{p} is not linearly controllable for the total force f and the moment M, the controller of a quadrotor is separated to a trajectory control loop and an attitude control loop.

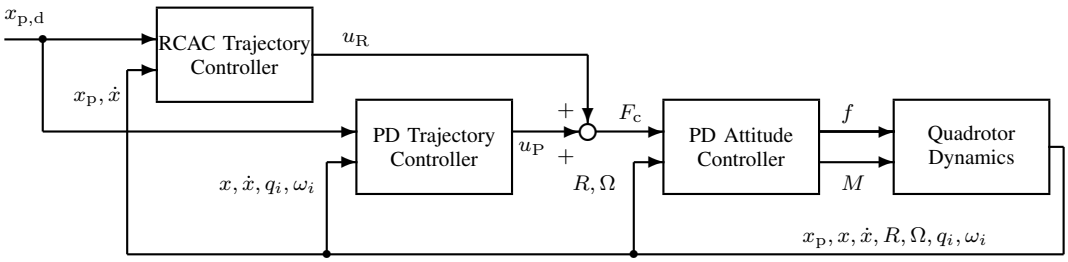

Fig. 2. Closed-loop quadrotor system. The measurements needed by the control system are $x_{\rm p}$, x, $\dot{x}$, R, Ω, q_i, and ω_i, for all $i \leq n$. Note that $x_{\rm p}$ can be calculated from x and q_i using knowledge of the length of each link. $x_{\rm p}$ and $\dot{x}$ are used for feedback in the RCAC trajectory controller. x, $\dot{x}$, q_i, and ω_i for all $i \leq n$ are used for feedback in the PD trajectory controller. R and Ω are used for feedback in the PD attitude controller.

To achieve the control objective, the trajectory control loop directly use the total thrust as the command to be designed. A simplified dynamic model is first derived for the design of the trajectory control loop. In this loop, a PD controller is designed to make the hanging equilibrium asymptotically stable for x, $\dot{x}$, q_i and ω_i with a nominal payload mass. The RCAC controller is then designed to compensate for the payload mass uncertainty.

To point the propellers to the proper direction to achieve the thrust command given by the trajectory control loop, the attitude control loop uses f and M as the command to be designed. In this loop, a geometric nonlinear PD controller is designed to achieve asymptotic tracking of the thrust command. The control architecture is given by Figure 2.

A. Simplified Dynamic Model

For the given equations of motion (4), the control thrust is given by $-fRe_3$. This implies that the total thrust magnitude f can be arbitrarily chosen, but the direction of the thrust vector is always along the third body-fixed axis. Also, the rotational attitude dynamics of the quadrotor are not affected by the translational dynamics of the quadrotor or the dynamics of links. Therefore, we replace the term $-fRe_3$ in (4) with $F \triangleq [F_1 \;\; F_2 \;\; F_3]^{\rm T} \in \mathbb{R}^3$, as shown in (20). Note that the simplified dynamics (20) are independent of the quadrotor attitude dynamics given by (3). This is equivalent to separating the dynamics into an outer loop, where the attitude R is assumed to be instantaneously achievable, and an inner loop that controls the attitude R.

The simplified dynamics are given by

$$\begin{bmatrix} m_{00} & m_{01} & m_{02} & \cdots & m_{0n} \\ -\hat{q}_1^2 m_{10} & m_{11} I_3 & -m_{12}\hat{q}_1^2 & \cdots & -m_{1n}\hat{q}_1^2 \\ -\hat{q}_2^2 m_{20} & -m_{21}\hat{q}_2^2 & m_{22} I_3 & \cdots & -m_{2n}\hat{q}_2^2 \\ \vdots & \vdots & \vdots & & \vdots \\ -\hat{q}_n^2 m_{n0} & -m_{n1}\hat{q}_n^2 & -m_{n2}\hat{q}_n^2 & \cdots & m_{nn} I_3 \end{bmatrix} \begin{bmatrix} \ddot{x} \\ \ddot{q}_1 \\ \ddot{q}_2 \\ \vdots \\ \ddot{q}_n \end{bmatrix} = \begin{bmatrix} F + m_{00} g e_3 \\ -\|\dot{q}_1\|^2 m_{11} q_1 - \sum_{a=1}^{n} m_a g l_1 \hat{q}_1^2 e_3 \\ -\|\dot{q}_2\|^2 m_{22} q_2 - \sum_{a=2}^{n} m_a g l_2 \hat{q}_2^2 e_3 \\ \vdots \\ -\|\dot{q}_n\|^2 m_{nn} q_n - m_n g l_n \hat{q}_n^2 e_3 \end{bmatrix}. \tag{20}$$

B. PD Trajectory Controller

In this subsection, a fixed-gain PD trajectory controller is designed to make states of the simplified dynamic asymptotically converge to the hanging equilibrium, where $x = x_{\rm p,d} - \sum_{i=1}^{n} l_i e_3$, $\dot{x} = 0_{3\times 1}$ and, for all $i \leq n$, $\omega_i = 0_{3\times 1}$ and $q_i = e_3$. Note the PD trajectory controller is designed for a nominal payload mass. We define the nominal payload mass as $\bar{m}_n$, and define the payload mass uncertainty as $\tilde{m}_n \triangleq m_n - \bar{m}_n$.

The control from the PD trajectory controller is given by

$$\begin{aligned} u_{\rm P} = &- K_x e_x - K_{\dot{x}} e_{\dot{x}} - \sum_{i=1}^{n} K_{\omega_i} e_{\omega_i} \\ &- \sum_{i=1}^{n} K_{q_i} e_{q_i} - (m_{00} - \tilde{m}_n) g e_3, \end{aligned}$$

where

$$\begin{aligned} e_x \triangleq x - x_{\rm p,d} + \sum_{i=1}^{n} l_i e_3, \;\; e_{\dot{x}} \triangleq \dot{x}, \\ e_{\omega_i} \triangleq [e_1 \;\; e_2]^T \omega_i, \;\; e_{q_i} \triangleq [e_1 \;\; e_2]^T (e_3 \times q_i). \end{aligned}$$

Note $m_{00} - \tilde{m}_n$ is the total mass of the quadrotor and links with a nominal payload mass.

C. RCAC Trajectory Controller

In this subsection, an RCAC trajectory controller is designed to compensate for the payload mass uncertainty. Since RCAC is used only for z axis, the control is given by $u_{\rm R}(k) \triangleq [0 \; 0 \; u_{{\rm R},3}(k)]^{\rm T}$. We define the performance vector for RCAC as

$$z(k) \triangleq \begin{bmatrix} \tilde{x}_{{\rm p},3}(k) \\ \dot{x}_3(k) \end{bmatrix} \in R^2, \tag{21}$$

where $\tilde{x}_{{\rm p},3}$ is the third entry of the payload position error

$$\tilde{x}_{\rm p}(k) \triangleq x_{\rm p}(k) - x_{\rm p,d}. \tag{22}$$

The parameters H_i for RCAC is obtained from the impulse response of (20) and (2) with $\tilde{m}_n = 0$ and the initial condition given by $x(0) = x_{\rm p,d} - \sum_{i=1}^{n} l_i e_3$, $\dot{x}(0) = 0_{3\times 1}$,

for all j, $q_j(0) = e_3$ and $\omega_j(0) = 0_{3\times 1}$. Specifically, for all $k \le n_{\rm f}$, we define

$$H_k \triangleq z(k), \tag{23}$$

where $z(k) \in \mathbb{R}^2$ is the column performance vector with the unit impulse input to the third channel with PD trajectory controller in the loop. Thus, the input used to obtain $z(k)$ can be given by $F_{\rm c}(0) = u_{\rm P}(0) + e_3$, $F_{\rm c}(1) = u_{\rm P}(1)$, $F_{\rm c}(2) = u_{\rm P}(2)$, …, $F_{\rm c}(n_{\rm f}) = u_{\rm P}(n_{\rm f})$. This is shown in Figure 3.

The thrust command $u_{{\rm R},3}(k) \in \mathbb{R}$ is calculated from the RCAC algorithm given by (11),(14),(18), and (19).

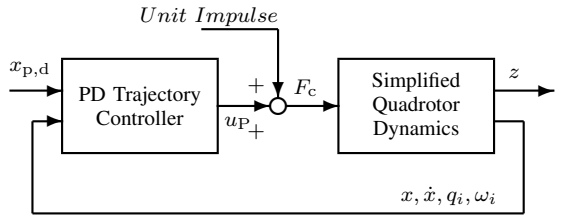

Fig. 3. Method for obtaining H_i. Note that the PD trajectory controller is in the loop. x, $\dot{x}$, q_i, and ω_i for all $i \le n$ are used for feedback in the PD trajectory controller. Note that the attitude controller and quadrotor dynamics are replaced by the simplified dynamics given by (2) and (20).

D. Attitude Controller

In this subsection, a fixed-gain geometric nonlinear PD controller is designed to asymptotically follow the total thrust command $F_{\rm c} \in \mathbb{R}^3$. The thrust command on the step k is given by

$$F_{\rm c} = u_{\rm R}(k) + u_{\rm P}(k). \tag{24}$$

The desired direction of the third body-fixed axis is given by

$$b_{3_d} = -\frac{F_{\rm c}}{\|F_{\rm c}\|}. \tag{25}$$

There is an additional one-dimensional degree of freedom of the quadrotor attitude that corresponds to the rotation about the third body-fixed axis. To resolve it, the desired direction of the first body-fixed axis, namely, $b_{1_d} \in \mathsf{S}^2$ is chosen to be the initial first body-fixed axis b_{1_0}.

The corresponding desired attitude is chosen as

$$R_{\rm d} = \begin{bmatrix} -\dfrac{\hat{b}^2_{3_d} b_{1_d}}{\|\hat{b}^2_{3_d} b_{1_d}\|} & \dfrac{\hat{b}_{3_d} b_{1_d}}{\|\hat{b}_{3_d} b_{1_d}\|} & b_{3_d} \end{bmatrix}, \tag{26}$$

which is in $\mathsf{SO(3)}$. The desired angular velocity is obtained by the attitude kinematics equation

$$\Omega_d = (R_{\rm d}^T \dot{R}_{\rm d})^\vee. \tag{27}$$

Next, we define the tracking error variables for the attitude and the angular velocity as

$$e_R \triangleq \frac{1}{2}(R_{\rm d}^T R - R^T R_{\rm d})^\vee, \tag{28}$$

$$e_\Omega \triangleq \Omega - R^T R_{\rm d} \Omega_d. \tag{29}$$

The thrust magnitude command and the moment command vector of quadrotor are chosen as

$$f_c = -F_c \cdot R e_3, \tag{30}$$

$$M_c = -K_R e_R - K_\Omega e_\Omega + \Omega \times J\Omega - J(\hat{\Omega} R^T R_{\rm d} \Omega_d - R^T R_{\rm d} \dot{\Omega}_d), \tag{31}$$

where $K_R \triangleq \omega_n^2 \|J\|$ and $K_\Omega \triangleq 2\omega_n \zeta \|J\|$, where ω_n and ζ are positive.

V. Numerical Examples

The desirable properties of the proposed control system are illustrated by some numerical examples. The sample time for each example is chosen as 0.01 sec. Properties of the quadrotor are chosen as

$$m = 0.5\,{\rm kg}, \quad J = {\rm diag}[0.557\ 0.557\ 1.05] \times 10^{-2}\,{\rm kgm}^2.$$

Three identical links with $n = 3$, $m_i = 0.1\,{\rm kg}$, and $l_i = 0.2\,{\rm m}$ are considered in the case with a nominal payload mass. The payload mass uncertainty is $\tilde{m}_3 = 0.1\,{\rm kg}$, thus $m_3 = 0.2\,{\rm kg}$ with the actual payload mass. Four rotors with maximum thrust $5\,{\rm N}$, $d = 0.2\,{\rm m}$, and $c_{\tau f} = 0.01\,{\rm m}$ are used as actuators.

The desired location of the payload is selected as $x_{\rm p,d} = 0_{3\times 1}$. The initial conditions for the quadrotor are given by

$$x(0) = [0.6\ \ -0.7\ \ 0.2]^{\rm T},\ \ \dot{x}(0) = 0_{3\times 1},$$
$$R(0) = I_3, \quad \Omega(0) = 0_{3\times 1}.$$

The initial direction of the links are chosen such that the cable is curved along the horizontal direction, as illustrated at Figure 4, and the initial angular velocity of each link is chosen as zero.

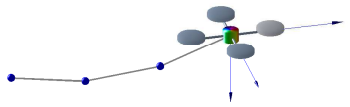

Fig. 4. Initial state of the links

The parameters of the RCAC trajectory controller are chosen as

$$n_c = 2,\ n_{\rm f} = 30,\ R_\Theta = 0.1 I_7,$$
$$R_z = {\rm diag}[1\ 0.1], \lambda = 1.$$

The parameters of the PD trajectory controller are chosen as

$$K_x = I_3,\ K_{\dot{x}} = {\rm diag}[1.75\ 1.75\ 1.67],$$

$$K_{q_1} = \begin{bmatrix} 0 & -4.8 \\ 4.8 & 0 \\ 0 & 0 \end{bmatrix}, K_{\omega_1} = \begin{bmatrix} 0 & -0.6 \\ 0.6 & 0 \\ 0 & 0 \end{bmatrix},$$

$$K_{q_2} = \begin{bmatrix} 0 & 3.8 \\ -3.8 & 0 \\ 0 & 0 \end{bmatrix}, K_{\omega_2} = \begin{bmatrix} 0 & -0.02 \\ 0.02 & 0 \\ 0 & 0 \end{bmatrix},$$

$$K_{q_3} = \begin{bmatrix} 0 & -0.2 \\ 0.2 & 0 \\ 0 & 0 \end{bmatrix}, K_{\omega_3} = \begin{bmatrix} 0 & -0.006 \\ 0.006 & 0 \\ 0 & 0 \end{bmatrix}.$$

The parameters of the PD attitude controller are chosen as

$$\omega_n = 10 \text{ rad/sec}, \ \zeta = 0.707.$$

A saturation block is added for the moment command. The amplitude limit for M_1 and M_2 is chosen as 1 N-m, and the amplitude limit for M_3 is chosen as 0.01 N-m.

To show the stabilizing performance for the links, we define the error functions

$$e_q \triangleq \sum_{i=1}^{n} \|q_i - e_3\|, \quad e_\omega \triangleq \sum_{i=1}^{n} \|\omega_i\|. \tag{32}$$

A. PD controller

In this example, RCAC controller is turned off. Therefore $F_c(k) = u_{\rm P}(k)$. Figure 5 shows that the closed-loop is stable and links are aligned in the vertical direction, but there is a asymptotic error about 1 m along the z axis.

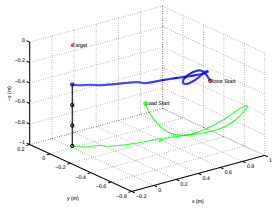

(a) 3D trace of the quadrotor translation (thick line) and the payload (thin line)

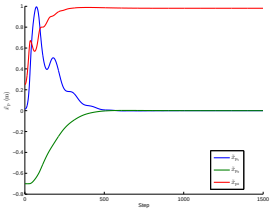

(b) Position error $\tilde{x}_{\rm p}$ of the payload

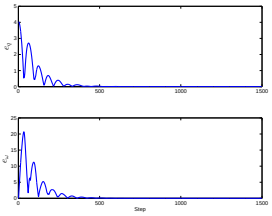

(c) Direction error e_q and angular velocity error e_ω for links

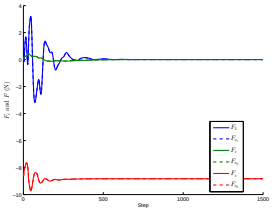

(d) Total force command F_c and actual total force F

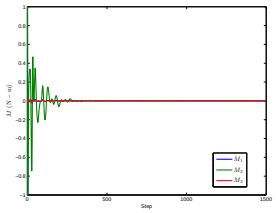

(e) Moment

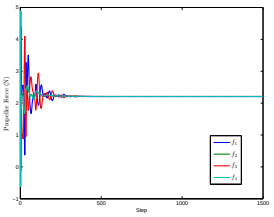

(f) Thrust for each propeller

Fig. 5. PD example. (a) shows that the close-loop is stable, (c) shows that the links are asymptotically aligned in the vertical direction and stop swinging in about 4 sec. However, (b) shows that there is a constant asymptotic error about 1 m along the z axis for $\tilde{m}_n = 0.1\,\text{kg}$. The asymptotic error is due to the extra gravity provided by the positive payload mass uncertainty.

B. PID controller

Since there is a large asymptotic error along the z axis in the example with PD controller alone, we add an extra integral term in the force command in this example to deal with the asymptotic error. Thus,

$$F_c(k) = u_{\rm P}(k) - \sum_{i=0}^{k} \begin{bmatrix} 0 & 0 & 0 \\ 0 & 0 & 0 \\ 0 & 0 & 0.25 \end{bmatrix} \tilde{x}_{\rm p}(k) T_{\rm s},$$

where $\tilde{x}_{\rm p}(k)$ is given by (22) and $T_{\rm s}$ is the sample time. Figure 6 shows that the asymptotic error along the z axis is slowly eliminated. Figure 6.(a) shows that the payload firstly arrive the position under the desired position and then go upward to arrive the desired position.

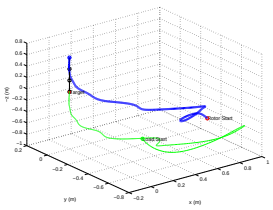

(a) 3D trace of the quadrotor translation (thick line) and the payload (thin line)

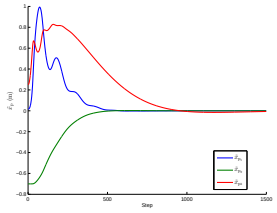

(b) Position error $\tilde{x}_{\rm p}$ of the payload

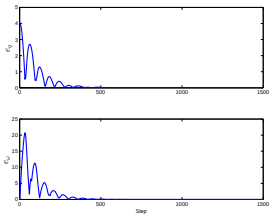

(c) Direction error e_q and angular velocity error e_ω for links

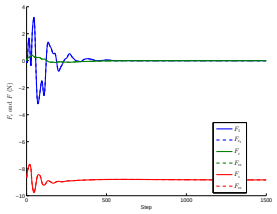

(d) Total force command F_c and actual total force F

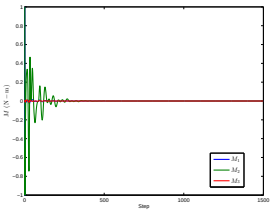

(e) Moment

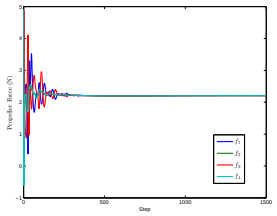

(f) Thrust for each propeller

Fig. 6. PID example. (b) shows that compared with the case with PD controller alone, the asymptotic error along the z axis is eliminated. (c) shows that the links are asymptotically aligned in the vertical direction and stop swinging in about 4 sec as in the PD example. (a) shows that the payload firstly arrive the position under the desired position and then go upward to arrive the desired position.

C. RCAC controller + PD Controller

In this example, RCAC controller is turned on, and thus $F_c(k) = u_{\rm P}(k) + u_{\rm R}(k)$. Figure 7 shows that the asymptotic error along the z axis is eliminated. Compared with the case with integral term in $F_c(k)$, the error along the z axis in this case converge faster and does not approach the desired position from the bottom but almost from the same horizontal plane.

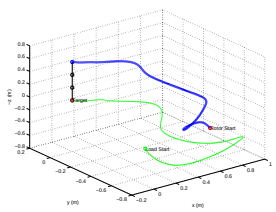

(a) 3D trace of the quadrotor translation (thick line) and the payload (thin line)

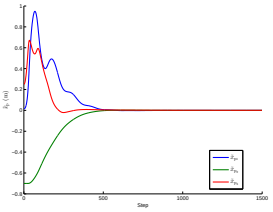

(b) Position error $\tilde{x}_{\mathrm{p}}$ of the payload

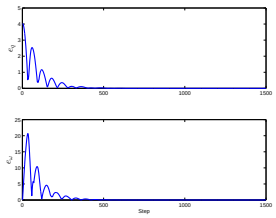

(c) Direction error e_q and angular velocity error e_ω for links

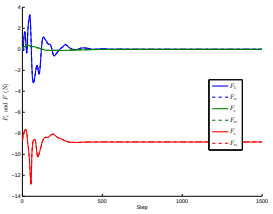

(d) Total force command F_c and actual total force F

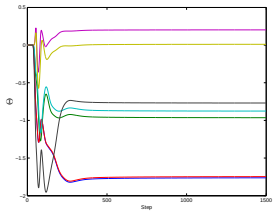

(e) Controller parameter $\Theta(k)$

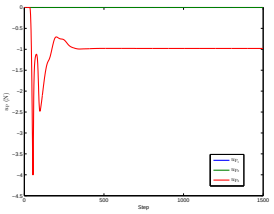

(f) Force command from RCAC trajectory controller u_{R}

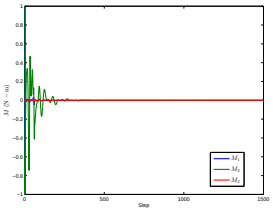

(g) Moment

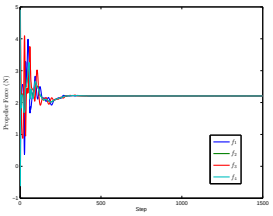

(h) Thrust for each propeller

Fig. 7. PD+RCAC example. (c) shows that the links are asymptotically aligned in the vertical direction and stop swinging in about 4 sec as in the PD and PID examples. (b) shows that compared with the case with integral term in $F_c(k)$, the error along the z axis in this case converge faster. (a) shows that the payload does not approach the desired position from the bottom but almost from the same horizontal plane.

VI. Conclusion

We design a tracking controller for a quadrotor UAV with a point-mass payload connected by a flexible cable modeled as the interconnection of rigid links.

A fixed-gain geometric nonlinear PD controller is first designed to achieve desired performance for a nominal payload mass. Enabled by the impulse response with PD controller in the loop, a retrospective cost adaptive controller is designed to compensate for the payload mass uncertainty in the case of aggressive maneuvers.

The performance of the combined controller is shown to achieve motion-to-rest maneuver, where the quadrotor and links have an arbitrary initial state and the objective is to transport the payload to a specified position while aligning the links in the vertical direction. Compared with the performance of the fixed-gain controller with an integral control term, the proposed controller have smaller settling time and overshoot.

Future research includes improved robustness to more types of uncertainties and disturbances, such as the uncertainty of quadrotor inertia, wind disturbance, and measurement noises. Aiming at rapid transportation of large sized payloads, a dynamic model that includes the rotation of the payload and interactions between the payload motion and the quadrotor motion is still under research. On the other hand, a model-free adaptive controller design method for a nonlinear system that only rely on the impulse response information from off-line or on-line identification is also under research.

References

[1] T. Lee, M. Leok, and N. McClamroch, "Geometric tracking control of a quadrotor UAV on SE(3)," in *Proceedings of the IEEE Conference on Decision and Control*, 2010, pp. 5420–5425.

[2] J. Gillula, H. Huang, M. Vitus, and C. Tomlin, "Design of guaranteed safe maneuvers using reachable sets: Autonomous quadrotor aerobatics in theory and practice," in *Proceedings of the International Conference on Robotics and Automation*, 2010, pp. 1649–1654.

[3] D. Mellinger, N. Michael, and V. Kumar, "Trajectory generation and control for precise aggressive maneuvers with quadrotors," *International Journal Of Robotics Research*, vol. 31, no. 5, pp. 664–674, 2012.

[4] L. Cicolani, G. Kanning, and R. Synnestvedt, "Simulation of the dynamics of helicopter slung load systems," *Journal of the American Helicopter Society*, vol. 40, no. 4, pp. 44–61, 1995.

[5] M. Bernard, "Generic slung load transportation system using small size helicopters," in *Proceedings of the International Conference on Robotics and Automation*, 2009, pp. 3258–3264.

[6] I. Palunko, P. Cruz, and R. Fierro, "Agile load transportation," *IEEE Robotics and Automation Magazine*, vol. 19, no. 3, pp. 69–79, 2012.

[7] N. Michael, J. Fink, and V. Kumar, "Cooperative manipulation and transportation with aerial robots," *Autonomous Robots*, vol. 30, pp. 73–86, 2011.

[8] I. Maza, K. Kondak, M. Bernard, and A. Ollero, "Multi-UAV cooperation and control for load transportation and deployment," *Journal of Intelligent and Robotic Systems*, vol. 57, pp. 417–449, 2010.

[9] K. Sreenath, T. Lee, and V. Kumar, "Geometric control and differential flatness of a quadrotor UAV with a cable-suspended load," in *Proceedings of the IEEE Conference on Decision and Control*, 2013, pp. 2269–2274.

[10] T. Lee, K. Sreenath, and V. Kumar, "Geometric control of cooperating multiple quadrotor UAVs with a suspended load," in *Proceedings of the IEEE Conference on Decision and Control*, 2013, pp. 5510–5515.

[11] F. A. Goodarzi, D. Lee, and T. Lee, "Geometric stabilization of a quadrotor uav with a payload connected by flexible cable," in *Proceedings of the American Control Conference*, 2014, accepted.

[12] J. B. Hoagg and D. S. Bernstein, "Retrospective cost model reference adaptive control for nonminimum-phase systems," *AIAA J. Guid. Contr. Dyn.*, vol. 35, pp. 1767–1786, 2012.

[13] J. B. Hoagg, M. A. Santillo, and D. S. Bernstein, "Discrete-time adaptive command following and disturbance rejection for minimum phase systems with unknown exogenous dynamics," *IEEE Trans. Autom. Contr.*, vol. 53, pp. 912–928, 2008.

[14] M. A. Santillo and D. S. Bernstein, "Adaptive control based on retrospective cost optimization," *AIAA J. Guid. Contr. Dyn.*, vol. 33, pp. 289–304, 2010.

[15] A. Morozov, J. B. Hoagg, and D. S. Bernstein, "Retrospective adaptive control of a planar multilink arm with nonminimum-phase zeros," in *Proceedings of the IEEE Conference on Decision and Control*, 2010, pp. 3706–3711.

[16] M. W. Isaacs, J. B. Hoagg, A. Morozov, and D. S. Bernstein, "A numerical study on controlling a nonlinear multilink arm using a retrospective cost model reference adaptive controller," in *Proceedings*

of the IEEE Conference on Decision and Control, 2011, pp. 8008–8013.

[17] G. Cruz and D. S. Bernstein, "Adaptive spacecraft attitude control with reaction wheel actuation," in *Proceedings of the American Control Conference*, 2013, pp. 4832–4837.

[18] G. Cruz, A. M. D'Amato, and D. Bernstein, "Retrospective cost adaptive control of spacecraft attitude," in *Proceedings of the AIAA Guidance, Navigation, and Control Conference*, 2012, AIAA-2012-4624.

[19] A. Tayebi and S. McGilvray, "Attitude stabilization of a VTOL quadrotor aircraft," *IEEE Transactions on Control System Technology*, vol. 14, no. 3, pp. 562–571, 2006.

[20] P. Castillo, R. Lozano, and A. Dzul, "Stabilization of a mini rotorcraft with four rotors," *IEEE Control System Magazine*, pp. 45–55, 2005.

[21] G. C. Goodwin and K. S. Sin, *Adaptive Filtering, Prediction, and Control*. Prentice Hall, 1984.